Multiple Structural Variants of $L_nCu^I(\mu\text{-}X)_2Cu^IL_n$ (n = 1, 2). Influence of Halide on a "Soft" Potential Energy Surface

Grigorii L. Soloveichik, Odile Eisenstein,* Jason T. Poulton, William E. Streib, John C. Huffman, and Kenneth G. Caulton*

Department of Chemistry and Molecular Structure Center, Indiana University, Bloomington, Indiana 47405, and Laboratoire de Chimie Theorique, Université de Paris-Sud, 91405 Orsay, France

Received December 10, 1991

The crystal structures of $Cu(PCy_3)_2I$ and $[Cu(PCy_3)I]_2$ are reported in order to furnish data to help understand the variation of Cu/Cu distances with changing halide in planar structures of the type $L_nCu^I(\mu\text{-}X)_2Cu^IL_n$ (n = 1, 2). It is found that iodide shows a shorter Cu/Cu separation (2.89 Å) than does chloride (3.07 Å) in $[Cu(PCy_3)X]_2$ species. An extended Hückel analysis of the bonding in these molecules indicates the Cu^I s and p orbitals to be most important in bonding and shows larger Cu/Cu overlap populations for the stronger donor (iodide over chloride). This is traced to weak σ and π Cu/Cu bonding interactions. Such bonding interaction is diminished when the terminal phosphine ligand is replaced by a π-donor (halide), in agreement with literature data for $Cu_2X_4^{2-}$ species. Analogous weakening is effected by addition of another terminal ligand to each copper (i.e., $L_2Cu^I(\mu\text{-}X)_2Cu^IL_2$). The geometry within the $Cu(\mu\text{-}X)_2Cu$ rhombus is shown to exist in a broad potential energy well, and diminished Cu/Cu interactions (i.e., longer Cu/Cu distances) are compensated by improved interaction of halide orbitals with in-plane out-of-phase Cu/Cu orbitals. This explains the surprisingly large in-plane distortions observed for $Cu_2X_4^{2-}$ species in solids containing various cations and in $L_2Cu(\mu\text{-}X)_2CuL_2$. Crystallographic data: for $Cu(PCy_3)_2I$ (at −174 °C), a = 9.634 (2) Å, b = 22.975 (5) Å, c = 9.058 (2) Å, α = 97.38 (1)°, β = 114.49 (1)°, and γ = 93.40 (1)° with Z = 2 in space group $P\bar{1}$; for $[Cu(PCy_3)I]_2$ (at −172 °C), a = 9.757 (2) Å, b = 12.780 (3) Å, c = 8.808 (2) Å, α = 94.26 (1)°, β = 116.74 (1)°, and γ = 96.37 (1)° with Z = 1 (dimer) in space group $P\bar{1}$.

Introduction

The chemistry of Lewis base adducts of copper(I) halides (X) is extremely rich and yields a large number of structural types.[1] However, only very bulky ligands form uncharged dimeric complexes $LCu(\mu\text{-}X)_2CuL$. Ionic salts of empirical formula M^ICuX_2 also contain the dimeric anions $XCu(\mu\text{-}X)_2CuX^{2-}$. In most cases, the distance between copper centers is anomalously short (down to 2.4 Å)[2a] or at least comparable to the sum of the covalent radii.[2b] The matter of metal/metal interactions (bonding) between two d^{10} electron configurations continues to challenge. For two Cu(I) centers, Cu/Cu separations range as small as 2.4 Å, with *many* examples of separation comparable to that (2.55 Å) in copper metal. An examination of the data available[2-15] for $XCu(\mu\text{-}X)_2CuX^{2-}$ species (Table I) shows no clearly discernible dependence of Cu/Cu distance on halide identity.[16] Several authors[17] have analyzed Cu^I_2 species and conclude that Cu/Cu bonding can exist where copper 4s and 4p orbitals convert the antibonding situation in A into the bonded case of B (i.e., $E_B < E_A$). (The drawing illustrates a σ-type interaction.)

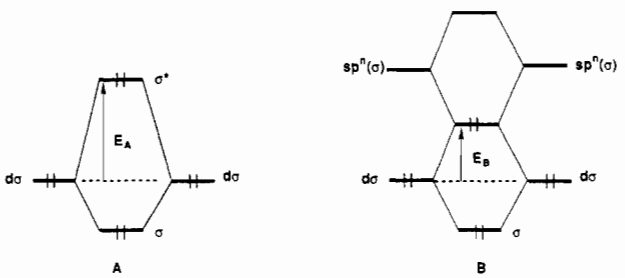

G.L.S. has studied for some time the adducts formed between Cp_2MH_n and CuX (X = Cl, I). These are of general formula $[Cp_2MH_n(CuX)_m]_2$ and sometimes incorporate $Cu(\mu\text{-}X)_2Cu$ substructures.[18,19] The Cu/Cu distances in such compounds

* To whom correspondence should be addressed: O.E., Université de Paris-Sud; K.G.C., Indiana University.

(1) Caulton, K. G.; Davies, G.; Holt, E. M. *Polyhedron* **1990**, *9*, 2319.
(2) (a) Haasnot, J. G.; Favre, T. L. T.; Hinrichs, W.; Reedijk, J. *Angew. Chem., Int. Ed. Engl.* **1988**, *27*, 856. (b) A covalent radius of 1.27 Å for Cu^I is available from the 2.04-Å Cu–C distance of $(Ph_3P)_3Cu\text{–}CH_3$, after subtracting the carbon covalent radius of 0.77 Å: Coan, P. S.; Folting, K.; Huffman, J. C.; Caulton, K. G. *Organometallics* **1989**, *8*, 2724.
(3) Banci, L.; Bencini, A.; Dei, A.; Gatteshi, D. *Inorg. Chim. Acta* **1984**, *84*, L11.
(4) Jagner, S. Personal communication.
(5) Churchill, M. R.; Rotella, F. J. *Inorg. Chem.* **1979**, *18*, 166.
(6) Shibaeva, R. P.; Kaminskii, V. K. *Kristallografiya* **1981**, *26*, 332. In some cases, the presence of short cation–anion contact has less effect on the geometry of the rhombus; see ref 8.
(7) Andersson, S.; Jagner, S. *Acta Chem. Scand.* **1985**, *A39*, 423.
(8) Canty, A. J.; Engelhardt, M. L.; Healy, P. C.; Kildea, J. D.; Minchin, N. J.; White, A. H. *Aust. J. Chem.* **1987**, *40*, 1881.
(9) Asplund, M.; Jagner, S. *Acta Chem. Scand.* **1984**, *A38*, 135.
(10) Asplund, M.; Jagner, S. *Acta Chem. Scand.* **1984**, *A38*, 411.
(11) Asplund, M.; Jagner, S.; Nilsson, M. *Acta Chem. Scand.* **1982**, *A36*, 754.
(12) Hartl, H.; Brudgam, I.; Mahdjour-Hassan Abadi, F. Z. *Naturforsch.* **1985**, *B40*, 1032.
(13) Healy, P. C.; Pakawatchai, C.; Raston, C. L.; Skelton, B. W.; White, A. H. *J. Chem. Soc., Dalton Trans.* **1983**, 1905.
(14) Dyason, J. C.; Engelhardt, L. M.; Healy, P. C.; Pakawatchai, C.; White, A. H. *Inorg. Chem.* **1985**, *24*, 1950.
(15) Hengefeld, A.; Kopf, J.; Nast, R. *Chem. Ber.* **1977**, *110*, 3078.
(16) There is no evidence in these data that trends in Cu/Cu separation are controlled by simple "mechanical" characteristics such as Cu–X or X···X distances or "preferred" angles at the bridging halide.
(17) (a) Mehrotra, P. M.; Hoffmann, R. *Inorg. Chem.* **1978**, *17*, 2187. (b) Merz, K. M., Jr.; Hoffmann, R. *Inorg. Chem.* **1988**, *27*, 2120. For an analysis of Cu–Cu interactions in chain systems, see: Cui, C. X.; Kertesz, M. *Inorg. Chem.* **1990**, *29*, 2568. (c) For a different point of view on Cu···Cu interactions, see: Avdeef, A.; Fackler, J. P., Jr. *Inorg. Chem.* **1978**, *17*, 2182. Lee, S. W.; Trogler, W. C. *Inorg. Chem.* **1990**, *29*, 1659. (d) For other discussions about d^{10}–d^{10} interactions, see: Dedieu, A.; Hoffmann, R. *J. Am. Chem. Soc.* **1978**, *100*, 2074. Mingos, D. M. P. *J. Chem. Soc., Dalton Trans.* **1976**, 1163. Rösch, N.; Görling, A.; Ellis, D. E.; Schmidbaur, H. *Angew. Chem., Int. Ed. Engl.* **1989**, *28*, 1357.
(18) Belsky, V. K.; Ishchenko, V. M.; Bulychev, B. M.; Soloveichik, G. L. *Polyhedron* **1984**, *3*, 749.
(19) Arkhireeva, T. M.; Bulychev, B. M.; Sizov, A. I.; Sokolova, T. A.; Belsky, V. K.; Soloveichik, G. L. *Inorg. Chim. Acta* **1990**, *169*, 109.

0020-1669/92/1331-3306$03.00/0

Table I. Bond Lengths (Å) and Angles (deg) for $L_nCu(\mu\text{-}X)_2CuL_n$ Species

X	L	cation	Cu–L	Cu–X	Cu–X′	Cu···Cu	X···X′	XCuX	CuXCu	ref
				A. Planar $LCu(\mu\text{-}X)_2CuL$						
Cl	Cl^-	$Cu_4Cl_2L_4^{2+}$	2.12	2.37	2.37	2.43	4.06	118.2	61.8	2
Cl	Cl^-	$VOsalen^+$	2.16	2.22	2.43	3.09	3.48	96.8	83.6	3
Cl	Cl^-	PEt_4^+	2.11	2.14	2.92	3.52	3.72	93.4	86.6	4
Cl	PCy_3		2.18	2.29	2.32	3.07	3.44	96.6	83.4	5
Br	Br^-	TTT^+	2.33	2.47	2.49	2.66	4.19	115.4	64.7	6
Br	Br^-	$NPhMe_3^+$	2.31	2.42	2.42	2.74	3.99	111.1	68.9	7
Br	Br^-	$(MeCN)CuN_3^+$	2.27	2.44	2.44	2.77	4.01	110.8	69.2	8
Br	Br^-	NEt_4^+	2.32	2.44	2.45	2.94	3.91	106.3	73.7	9
I	I^-	NPr_4^+	2.50	2.57	2.58	2.70	4.39	116.9	63.1	10
I	I^-	NBu_4^+	2.51	2.57	2.59	2.73	4.38	116.2	63.8	11
I	I^-	$(MeCN)CuN_3^+$	2.52	2.55	2.56	2.78	4.28	114.0	66.0	8
I	I^-	PPh_4^+	2.50	2.58	2.60	2.96		110.3	69.4	12
I	2,6-Me_2pip		2.12	2.51	2.65	2.54	4.49	121.2	58.8	13
I	PCy_3		2.23	2.56	2.58	2.89	4.25	111.5	68.5	this work
				B. $L_2Cu(\mu\text{-}X)_2CuL_2$						
Cl	2,4-Me_2py		2.02	2.46	2.48	2.99	3.93	105.3	74.7	14
Br	2,4-Me_2py		2.03	2.58	2.50	3.09	4.16	106.7	73.3	14
I	2,4-Me_2py		2.03, 2.05	2.70	2.73	3.14	4.43	109.3	70.7	14
I	$P(CCPh)_3$		2.25	2.62	2.64	2.87	4.41	113.9	66.1	15
			2.26	2.61	2.63	2.74	4.47	116.8	63.2	

correlate primarily with the copper coordination number, being shorter when the copper is three- rather than four-coordinate.[19] However, the influence of the identity of the halide on the Cu/Cu distance in these compounds remains confusing. The structure of the $Cu_2X_4^{2-}$ ions will reflect the composite influence of variation of both terminal and bridging donor ligand capacity.[20] We therefore sought to examine a simpler structural type. Moreover, since the $Cu_2X_4^{2-}$ structure can vary as the cation is changed,[2-4,6-12] we decided to investigate uncharged molecules. We therefore address the present report to a simpler class of molecules and ask the following questions: (1) How does the Cu/Cu separation vary with X for the molecules $Cu_2(\mu\text{-}X)_2(PR_3)_2$? (2) What is the origin of this effect? We will show how the results obtained for this series can help understand the wide range of structures shown in Table I for $L_nCu^I(\mu\text{-}X)_2Cu^IL_n$ (n = 1, 2).

Experimental Section

All manipulations employed Schlenk techniques under an N_2 atmosphere. NMR spectra were recorded on a Nicolet NT-360 instrument.

Both phosphine complexes were synthesized from CuI and PCy_3 ($^{31}P\{^1H\}$ NMR chemical shift is 10.30 ppm in C_6D_6) according to the literature procedure.[21]

The compound $[Cu(PCy_3)I]_2$ is insoluble in common organic solvents at 25 °C but more soluble in hot aromatic hydrocarbons. NMR spectra (δ; 360 MHz, C_6D_6, 55 °C): ^1H, 2.20, 2.04, 1.99, 1.76, 1.68, 1.57, 1.35, 1.29, 1.16; $^{31}P\{^1H\}$, 9.44. Colorless single crystals, used in the structure determination, were obtained by slow cooling of a hot solution of $[Cu(PCy_3)_2I]_2$ in toluene/acetonitrile (1:1).

The compound $Cu(PCy_3)_2I$ was obtained as two apparently distinct polymorphs. Crystals obtained from a THF/pentane solvent mixture were unsuitable for X-ray data collection. On further standing for 72 h in their mother liquor, these crystals recrystallized into a pale amber polymorph; the latter were used for the X-ray structure determination. NMR spectra (δ; 360 MHz, C_6D_6, 25 °C): ^1H, 2.14, 2.10, 2.04, 2.01, 1.74, 1.72, 1.66, 1.63, 1.60, 1.30, 1.26, 1.23, 1.21, 1.16; $^{31}P\{^1H\}$, 10.93.

X-ray Diffraction Study of $[Cu(PCy_3)I]_2$. A small well-formed crystal was affixed to the end of a glass fiber and transferred to a goniostat where it was cooled to –172 °C for characterization and data collection (Table II). A systematic search of a limited hemisphere of reciprocal space located a set of diffraction maxima with no symmetry or systematic absences, indicating a triclinic space group. Subsequent solution and refinement confirmed this choice. The cell parameters were similar to those reported[5] for the chloride analog, but the differences were significant enough that there was some doubt as to whether or not the structures are isomorphous. For this reason, the reduced cell was chosen for the present structure (a permutation of the axes reported for the chloride). Data were collected ($6° < 2\theta < 45°$) using a moving-crystal/moving-detector technique[22] with fixed background counts at each extreme of the scan. After correction for Lorentz and polarization terms, equivalent data were averaged (R = 0.019). The structure was solved by a combination of direct methods and Fourier techniques. All hydrogen atoms were clearly visible in a difference Fourier map phased on the non-hydrogen atoms and were included in the final least-squares refinement. An absorption correction was applied prior to the final least-squares cycles (maximum and minimum absorptions 0.85 and 0.91). A final difference Fourier map was featureless; the largest peak was near the iodine atom (0.85 e/Å^3, minimum –0.73 e/Å^3). The results are shown in Tables III and IV and Figure 1.

Table II. Crystallographic Data for $[Cu(PCy_3)I]_2$

chem formula	$C_{36}H_{66}Cu_2I_2P_2$	Z	1
space group	$P\bar{1}$	fw	941.77
a, Å	9.757 (2)	T, °C	–172
b, Å	12.780 (3)	λ, Å	0.710 69
c, Å	8.808 (2)	ρ_{calcd}, g cm^{-3}	1.620
α, deg	94.26 (1)	μ(Mo Kα), cm^{-1}	27.9
β, deg	116.74 (1)	R	0.0313
γ, deg	96.37 (1)	R_w	0.0334
V, Å^3	965.21		

X-ray Structure Determination of $Cu(PCy_3)_2I$. A crystal of suitable size was obtained by cleaving a large piece of the sample in a nitrogen atmosphere glovebag. The crystal was mounted using silicone grease, and it was then transferred to a goniostat where it was cooled to –174 °C for characterization and data collection (Table V). A systematic search of a limited hemisphere of reciprocal space revealed no symmetry among the observed intensities. An initial choice of space group $P\bar{1}$ was later proven correct by the successful solution of the structure. Following complete intensity data collection ($6° < 2\theta < 45°$) and correction for absorption, data processing gave a residual of 0.020 for the averaging of 3273 unique intensities which had been measured more than once. Four standards measured every 400 data showed no significant trends. The structure was solved using a combination of direct methods (SHELXS-86) and Fourier techniques. The positions of the heavy atoms, I, Cu, and P, were determined from subsequent iterations of least-squares refinement and difference Fourier calculation. Hydrogens were included in fixed-calculated positions with thermal parameters fixed at 1 Å^2 plus the isotropic thermal parameter of the atom to which they were bonded. In the final cycles of refinement, the non-hydrogen atoms were varied with anisotropic thermal parameters. The final difference map was essentially featureless, the largest peak being 0.55 e/Å^3 and the largest hole –0.56 e/Å^3. The results are shown in Tables VI and VII and Figures 2 and 3.

Results

Structure Determinations. (a) $[Cu(PCy_3)I]_2$. In the solid state, $Cu(PCy_3)I$ is composed of centrosymmetric dimers separated

(20) Certain of these species are folded about the X···X axis. We will limit our discussions to the subgroup of molecules containing a planar Cu_2X_2 rhombus.

(21) Moers, F. G.; Op Het Veld, P. H. *J. Inorg. Nucl. Chem.* **1970**, *32*, 3225.

(22) Huffman, J. C.; Lewis, L. N.; Caulton, K. G. *Inorg. Chem.* **1980**, *19*, 2755.

Table III. Fractional Coordinates[a] and Isotropic Thermal Parameters[b] for $[Cu(PCy_3)I]_2$

	x	y	z	$10B_{iso}$, Å^2
I(1)	9336.3 (5)	4065.3 (3)	1530.0 (5)	18
Cu(2)	10914 (1)	5805.9 (5)	1470 (1)	12
P(3)	12151 (2)	7083 (1)	3708 (2)	11
C(4)	12886 (6)	8325 (4)	3158 (7)	14
C(5)	14182 (7)	8144 (5)	2690 (8)	14
C(6)	14782 (7)	9142 (5)	2181 (8)	17
C(7)	13476 (7)	9560 (5)	749 (7)	16
C(8)	12195 (7)	9741 (5)	1215 (8)	15
C(9)	11585 (6)	8744 (4)	1699 (7)	13
C(10)	10883 (6)	7440 (4)	4659 (7)	12
C(11)	11263 (6)	8587 (4)	5580 (7)	13
C(12)	10182 (7)	8750 (5)	6355 (8)	16
C(13)	8477 (7)	8504 (5)	5018 (8)	17
C(14)	8097 (7)	7373 (5)	4104 (8)	17
C(15)	9170 (6)	7182 (5)	3323 (7)	15
C(16)	13885 (6)	6720 (4)	5492 (7)	13
C(17)	14771 (7)	7551 (5)	7075 (8)	20
C(18)	16226 (8)	7183 (5)	8380 (9)	28
C(19)	15843 (9)	6141 (5)	8917 (9)	28
C(20)	14943 (7)	5284 (5)	7340 (8)	19
C(21)	13487 (7)	5647 (5)	6002 (8)	16
H(1)	1331 (6)	877 (4)	412 (7)	3 (10)
H(2)	1506 (6)	795 (4)	369 (7)	5 (10)
H(3)	1381 (6)	764 (4)	177 (7)	1 (10)
H(4)	1524 (6)	960 (4)	309 (7)	0 (10)
H(5)	1558 (7)	898 (4)	186 (7)	11 (11)
H(6)	1380 (5)	1013 (4)	45 (6)	0 (10)
H(7)	1299 (7)	902 (5)	−34 (8)	21 (13)
H(8)	1242 (5)	1029 (4)	202 (7)	0 (9)
H(9)	1133 (7)	999 (4)	25 (8)	15 (11)
H(10)	1112 (6)	815 (4)	73 (7)	6 (10)
H(11)	1077 (6)	891 (4)	202 (6)	0 (9)
H(12)	1101 (5)	698 (4)	547 (6)	0 (9)
H(13)	1241 (7)	877 (4)	651 (7)	10 (11)
H(14)	1120 (6)	916 (4)	486 (7)	8 (10)
H(15)	1028 (6)	830 (5)	717 (7)	14 (12)
H(16)	1036 (5)	939 (4)	681 (6)	0 (10)
H(17)	777 (8)	866 (5)	548 (9)	33 (15)
H(18)	821 (6)	903 (4)	414 (7)	15 (12)
H(19)	823 (6)	687 (5)	496 (7)	16 (12)
H(20)	715 (7)	728 (4)	332 (7)	1 (10)
H(21)	899 (5)	765 (4)	242 (6)	0 (9)
H(22)	895 (5)	649 (4)	276 (6)	2 (9)
H(23)	1459 (6)	663 (4)	501 (7)	8 (10)
H(24)	1498 (5)	828 (4)	680 (6)	0 (9)
H(25)	1419 (7)	767 (4)	759 (7)	15 (13)
H(26)	1701 (7)	710 (5)	788 (8)	22 (13)
H(27)	1670 (8)	764 (5)	924 (9)	24 (15)
H(28)	1676 (7)	587 (5)	972 (8)	21 (13)
H(29)	1521 (9)	621 (6)	945 (10)	38 (18)
H(30)	1566 (6)	512 (4)	687 (6)	2 (9)
H(31)	1468 (7)	458 (5)	772 (7)	20 (12)
H(32)	1281 (6)	572 (4)	648 (7)	6 (10)
H(33)	1304 (6)	516 (4)	512 (7)	8 (11)

[a] Fractional coordinates are $\times 10^4$ for non-hydrogen atoms and $\times 10^3$ for hydrogen atoms. [b] Isotropic values for those atoms refined anisotropically are calculated using the formula given by: Hamilton, W. C. *Acta Crystallogr.* **1959**, *12*, 609.

Table IV. Selected Bond Distances (Å) and Angles (deg) for $[Cu(PCy_3)I]_2$

I(1)–Cu(2)	2.5619 (10)	P(3)–C(4)	1.855 (6)
I(1)′–Cu(2)	2.5787 (10)	P(3)–C(10)	1.855 (5)
Cu(2)–Cu(2)′	2.8925 (15)	P(3)–C(16)	1.854 (5)
Cu(2)–P(3)	2.2250 (16)		
Cu(2)′–I(1)–Cu(2)	68.48 (3)	I(1)′–Cu(2)–P(3)	124.93 (5)
I(1)–Cu(2)–I(1)′	111.52 (3)	Cu(2)′–Cu(2)–P(3)	175.66 (5)
I(1)–Cu(2)–Cu(2)′	55.48 (3)	Cu(2)–P(3)–C(4)	113.00 (19)
I(1)–Cu(2)′–Cu(2)	56.035 (27)	Cu(2)–P(3)–C(10)	111.89 (17)
I(1)–Cu(2)–P(3)	123.34 (5)	Cu(2)–P(3)–C(16)	113.72 (18)

from each other by normal van der Waals distances (Figure 1). The structure is extremely similar to that of the (centrosymmetric) chloride analog.[5] Both molecules adopt a rotational conformation about the P–Cu bond which eclipses one P–C bond (i.e., the cyclohexyl group containing C(4)) with the $Cu(\mu\text{-}X)_2$ plane. This in turn seems to control the conformation about that P–C bond so that the smaller (i.e., face) profile of the cyclohexyl ring opposes the bridging halide. The remaining cyclohexyl rings are rotated 90° about the P–C bond. All cyclohexyl rings adopt the chair conformation with P equatorial. The two independent Cu–(μ-I) distances are nearly identical (they differ by only 0.017 Å), and copper is coplanar with its three attached groups (the sum of angles around Cu is 359.79°). Phosphorus is nearly collinear with the Cu–Cu vector: the angle Cu–Cu–P is 175.66 (5)°. A major difference between the two $[Cu(PCy_3)X]_2$ structures is that the larger halide (iodide) has the shorter Cu/Cu separation. The iodide and chloride show Cu/Cu distances of 2.89 and 3.07 Å, and the Cu–(μ-X)–Cu angle is much more acute for the iodide (68.48 (3)°) than for the chloride (83.44 (7)°).

(b) $Cu(PCy_3)_2I$. $Cu(PCy_3)_2I$ (Figure 2) is a three-coordinate monomer in the solid state. The CuP_2I unit is planar (sum of angles at copper equals 359.9°), and the $Cu(PC_3)_2I$ unit closely approaches C_{2v} symmetry. Phosphorus occupies an equatorial site on each cyclohexyl chair, and only the rotational orientations of the cyclohexyl rings about the P–C bonds destroy the C_{2v} symmetry. The two I–Cu–P angles are quite similar (110.99 (3) and 114.79 (3)°) and are smaller than the P–Cu–P angle (134.06 (4)°), due to the greater bulk of the phosphine ligands. As shown in Figure 3, the metal center is too crowded to permit dimerization (or, more generally, coordination number 4), but the packing of the cyclohexyl rings is apparently quite efficient. This suggests that the α-modification of $CuI(PCy_3)_2$ previously described by Moers and Op Het Veld[21] cannot be a dimer. Indeed, their IR data were interpreted as indicating a terminal iodine atom (i.e., monomeric structure).[21] The larger size of PCy_3 is also evident in the larger P–Cu–P angle reported here, compared to the corresponding values for PPh_3 (126.9°) and PPh_2(*o*-tolyl) (126.4°) in their CuP_2I compounds.[23]

Influence of X→M Donation on Cu^I/Cu^I Interactions in $(R_3P)Cu(\mu\text{-}X)_2Cu(PR_3)$. Extended Hückel calculations[24] (EHT) were done on the model compounds $Cu_2X_2(PH_3)_2$ using the experimental geometry of $Cu_2Cl_2(PCy_3)_2$. Variation in the electron-donating capability of X was simulated by changing the energy (H_{pp}) of the p orbital of the bridging μ-X by 1 eV around the reference value for Cl (−14.2 eV). The total Cu···Cu overlap population was found positive (0.0143), even with the Cu/Cu distance fixed at 3.07 Å, and increased as the energy of H_{pp} increased from −15.2 (0.0128) to −13.2 eV (0.0159). These values for the overlap populations are comparable to those found in other Cu^I polynuclear complexes where Cu···Cu bonding was suggested to take place.[17] There is thus a clear indication of increased Cu···Cu interaction in the case of a better μ-X electron donor center (I vs Cl) in these systems. This accounts well for the shorter Cu···Cu distance in $Cu_2(\mu\text{-}I)_2(PCy_3)_2$ (2.89 Å) compared to $Cu_2(\mu\text{-}Cl)_2(PCy_3)_2$ (3.07 Å).[5] However, this does not explain the very large spectrum of Cu···Cu distances (see below and Table I) which has been observed in *other* dinuclear $L_nCu^I(\mu\text{-}X)_2Cu^IL_n$ species. The following discussion of the interactions at work in these systems will attempt to propose a rationale for this set of puzzling observations. We will start by discussing the orbital interactions in the case of $Cu_2(\mu\text{-}X)_2L_2$ (L

(23) (a) Bowmaker, G. A.; Dyason, J. C.; Healy, P. C.; Engelhardt, L. M.; Pakauatchai, C.; White, A. H. *J. Chem. Soc., Dalton Trans.* **1987**, 1089. (b) Bowmaker, G. A.; Engelhardt, L. M.; Healy, P. C.; Kildea, J. D.; Papasergio, R. I.; White, A. H. *Inorg. Chem.* **1987**, *26*, 3533.

(24) Extended Hückel calculations were done using the weighted H_{ij} formula: Ammeter, J. H.; Bürgi, H.-B.; Thibeault, J. C.; Hoffmann, R. *J. Am. Chem. Soc.* **1978**, *100*, 3686. The atomic parameters were taken from the literature. Cu: Hay, P. J.; Thibeault, J. C.; Hoffmann, R. *J. Am. Chem. Soc.* **1975**, *97*, 4884. Cl and P: Summerville, R. H.; Hoffmann, R. *J. Am. Chem. Soc.* **1976**, *98*, 7240.

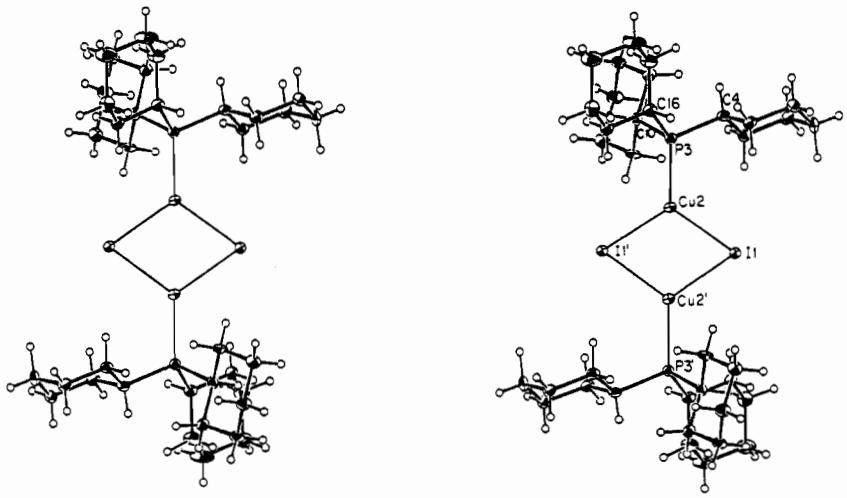

Figure 1. Stereo ORTEP drawing of $[Cu(PCy_3)I]_2$, viewed perpendicular to the Cu_2I_2 plane.

Table V. Crystallographic Data for $Cu(PCy_3)_2I$

chem formula	$C_{36}H_{66}CuIP_2$	Z	2
space group	$P\bar{1}$	fw	751.32
a, Å	9.634 (2)	T, °C	−174
b, Å	22.975 (5)	λ, Å	0.710 69
c, Å	9.058 (2)	ρ_{calcd}, g cm^{-3}	1.390
α, deg	97.38 (1)	μ(Mo Kα), cm^{-1}	15.7
β, deg	114.49 (1)	R	0.0293
γ, deg	93.40 (1)	R_w	0.0320
V, Å^3	1795.23		

= phosphine) (**1**) and later proceed to enlarge our discussion to other systems, $Cu_2X_4^{2-}$ (**2**) and $L_2Cu^I(\mu\text{-}X)_2Cu^IL_2$ (**3**).

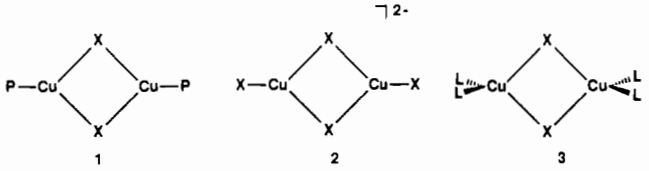

Earlier studies[17,25] (which did not examine μ-halide systems or the influence of various halides) have suggested that the occurrence of a bonding interaction between two d^{10} metal centers is due to the admixture of s and p orbitals of Cu into the d block, which decreases the four-electron destabilization as summarized in the Introduction. When such an admixture occurs, electron density is transferred from the d orbitals into the participating s and p orbitals. No such transfer is apparent in our calculations on $Cu_2X_2L_2$. The population of the d block is calculated to be a d^{10} situation, and furthermore no variation in the population of the d block is observed as the energy of the p orbitals of μ-X is varied. In contrast, significant changes in the Cu···Cu and Cu–X interactions involve direct electronic transfer from the orbitals of X into the s and p orbitals of Cu. A similar observation has been made by Hoffmann for a trinuclear Cu^I complex with bridging pentaazenido ligand.[17b] For this reason, we will concentrate our attention on the s and p orbitals of Cu and see how they respond to a change in the nature of μ-X.

The symmetry of the complex is D_{2h} if one neglects the cyclohexyl groups on the phosphines. For convenience, the p_x, p_y, and p_z orbitals of Cu and X will be named x, y, and z, respectively. Note that, besides the orbital describing the Cu–L bond, all other orbitals of Cu made from s and p orbitals are empty, since we are considering the bridged ligand as X^-. The schematic interaction diagram for $Cu_2(\mu\text{-}X)_2P_2$ as made from $Cu_2P_2^{2+}$ and X_2^{2-} fragments is shown in Figure 4.

Let us first describe the interaction involving the z orbitals, which are perpendicular to the molecular plane and form the purely π orbitals of the complex. The two z orbitals of Cu combine as π^+_z and π^-_z. One can form the same combinations z^+ and z^- from the z orbitals of the bridged X_2 unit. By symmetry only, π^+_z can interact with z^+, making an in-phase combination, z^+ +

Table VI. Fractional Coordinates and Isotropic Thermal Parameters[a] for $Cu(PCy_3)_2I$

	10^4x	10^4y	10^4z	$10B_{iso}$, Å^2
Cu(1)	3378 (1)	7500.4 (2)	5451 (1)	10
P(2)	3826 (1)	6640.7 (4)	6469 (1)	9
C(3)	5442 (5)	6738 (2)	8562 (5)	12
C(4)	6697 (5)	7232 (2)	8795 (5)	15
C(5)	7919 (5)	7365 (2)	10565 (5)	20
C(6)	8613 (5)	6813 (2)	11148 (5)	17
C(7)	7370 (5)	6325 (2)	10918 (5)	19
C(8)	6176 (5)	6183 (2)	9127 (5)	15
C(9)	4244 (4)	6037 (2)	5201 (5)	11
C(10)	5683 (5)	6228 (2)	4956 (5)	14
C(11)	6004 (5)	5746 (2)	3866 (5)	17
C(12)	4624 (5)	5569 (2)	2196 (5)	16
C(13)	3204 (5)	5357 (2)	2437 (5)	16
C(14)	2852 (5)	5834 (2)	3535 (5)	13
C(15)	2123 (4)	6306 (2)	6677 (5)	13
C(16)	2161 (5)	5693 (2)	7181 (5)	17
C(17)	626 (5)	5465 (2)	7160 (6)	21
C(18)	179 (5)	5899 (2)	8249 (6)	19
C(19)	152 (5)	6515 (2)	7758 (5)	18
C(20)	1686 (5)	6736 (2)	7802 (5)	15
P(21)	2749 (1)	8382.6 (4)	6315 (1)	9
C(22)	915 (4)	8270 (2)	6521 (5)	11
C(23)	−302 (5)	7829 (2)	5065 (5)	14
C(24)	−1726 (5)	7671 (2)	5349 (5)	14
C(25)	−2387 (5)	8219 (2)	5747 (5)	16
C(26)	−1177 (5)	8634 (2)	7233 (5)	16
C(27)	217 (4)	8817 (2)	6920 (5)	13
C(28)	2588 (4)	8911 (2)	4867 (5)	11
C(29)	1162 (5)	8727 (2)	3213 (5)	13
C(30)	1226 (5)	9083 (2)	1937 (5)	16
C(31)	1354 (5)	9744 (2)	2529 (5)	18
C(32)	2731 (5)	9936 (2)	4183 (5)	17
C(33)	2683 (4)	9572 (2)	5470 (5)	13
C(34)	4080 (5)	8818 (2)	8343 (5)	11
C(35)	5685 (4)	8964 (2)	8410 (5)	11
C(36)	6765 (5)	9343 (2)	10065 (5)	15
C(37)	6872 (5)	9038 (2)	11501 (5)	16
C(38)	5284 (5)	8892 (2)	11436 (5)	14
C(39)	4190 (5)	8512 (2)	9796 (5)	13
I(40)	3380.4 (3)	7476.4 (1)	2583.7 (3)	15

[a] Isotropic values for those atoms refined anisotropically are calculated using the formula given by: Hamilton, W. C. *Acta Crystallogr.* **1959**, *12*, 609.

(25) The complicated problem of the nature of metal–metal bonding in bridged transition metal systems has been addressed several times. See, for instance: Shaik, S.; Hoffmann, R. *J. Am. Chem. Soc.* **1980**, *102*, 1194. Shaik, S.; Hoffmann, R.; Fisel, C. R.; Summerville, R. H. *J. Am. Chem. Soc.* **1980**, *102*, 4555. Burdett, J. K. *J. Chem. Soc., Dalton Trans.* **1977**, 423.

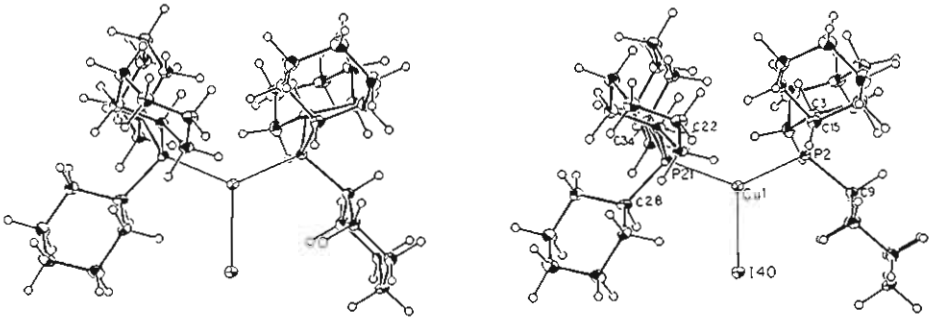

Figure 2. Stereo ORTEP drawing of $Cu(PCy_3)_2I$, viewed perpendicular to the CuP_2I plane. Only ipso-carbons are labeled.

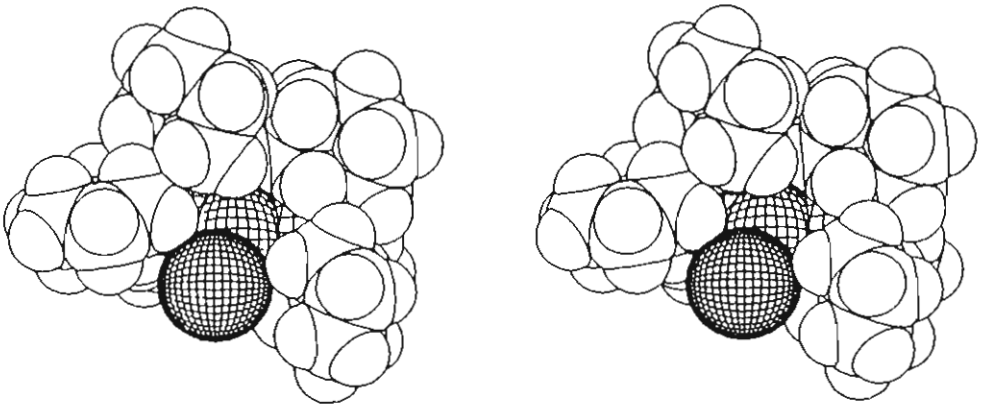

Figure 3. Stereo space-filling drawing of $Cu(PCy_3)_2I$. Copper and iodide are coarsely and finely cross hatched, respectively.

Table VII. Selected Bond Distances (Å) and Angles (deg) for $Cu(PCy_3)_2I$

I(40)–Cu(1)	2.5913 (7)	P(2)–C(15)	1.861 (4)
Cu(1)–P(2)	2.2753 (12)	P(21)–C(22)	1.859 (4)
Cu(1)–P(21)	2.2846 (12)	P(21)–C(28)	1.865 (4)
P(2)–C(3)	1.863 (4)	P(21)–C(34)	1.855 (4)
P(2)–C(9)	1.857 (4)		
I(40)–Cu(1)–P(2)	114.79 (3)	C(9)–P(2)–C(15)	103.68 (18)
I(40)–Cu(1)–P(21)	110.99 (3)	Cu(1)–P(21)–C(22)	110.56 (13)
P(2)–Cu(1)–P(21)	134.06 (4)	Cu(1)–P(21)–C(28)	111.02 (13)
Cu(1)–P(2)–C(3)	113.27 (14)	Cu(1)–P(21)–C(34)	118.73 (13)
Cu(1)–P(2)–C(9)	116.18 (13)	C(22)–P(21)–C(28)	109.93 (17)
Cu(1)–P(2)–C(15)	111.42 (14)	C(22)–P(21)–C(34)	102.98 (18)
C(3)–P(2)–C(9)	105.81 (18)	C(28)–P(21)–C(34)	103.03 (18)
C(3)–P(2)–C(15)	105.50 (18)		

π^+_z, mainly localized on the more electronegative partner, $(X)_2^{2-}$. The two other orbitals, π^-_z and z^-, cannot overlap. As the energy of the orbitals of the bridged atoms X is raised, there is more mixing between X_2^{2-} z^+ and $Cu_2P_2^{2+}$ π^+_z and therefore more electron density transferred into the metal fragment. This builds a weak bonding interaction between the two Cu z orbitals via π^+_z. This bonding is critically dependent upon copper being three-coordinated and planar, or what would conventionally be called coordinatively unsaturated.

While it is clear that the interaction of the z-type orbitals results in some Cu···Cu bonding, since, by symmetry, no electrons are transferred into π^-_z, the situation is considerably less clear for the other orbitals of Cu.[25]

In-phase and out-of-phase combinations of the Cu y orbitals can be formed. π^+_y interacts with the Cl_2 y^- orbital and π^-_y interacts with Cl_2 x^- orbital. Electron transfer from the chlorine into these two Cu_2 orbitals, π^+_y and π^-_y, leads to opposite effects: creation of a bond for π^+_y; annihilation of it for π^-_y. The first interaction dominates for an acute angle at X because of a larger overlap. For a more obtuse Cu–X–Cu angle and for the same Cu–X distances (thus a more acute X–Cu–X angle), the overlap between π^-_y (antibonding between metal centers) and x^- becomes increasingly important and no Cu···Cu bond is created. It is important to notice that both of these interactions contribute to the Cu–X bonds so that there is no significant total energy change with the variation of the Cu–X–Cu angle; the diminution of one interaction is compensated by the increase in the other one. Raising the energy of the orbitals of the bridged atoms increases the

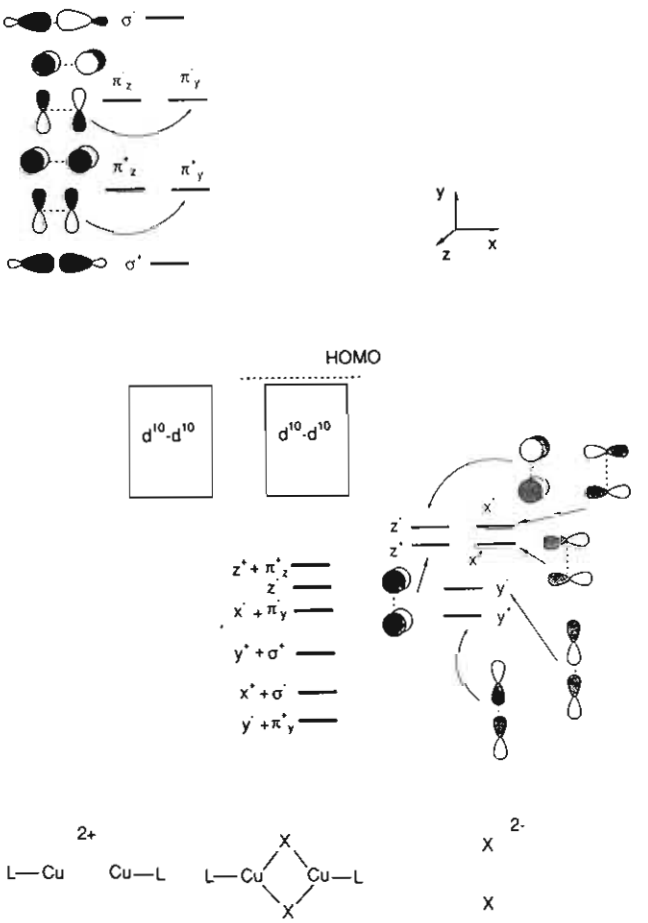

Figure 4. Interaction diagram for $(LCu\cdots CuL)^{2+}$ and X_2^{2-} fragments forming $LCu^I(\mu\text{-}X)_2Cu^IL$. The energy scale is not quantitative.

electron transfer from X into Cu, which can promote or diminish the formation of a Cu···Cu bond, depending on the value of the Cu–X–Cu angle.

The orbitals on Cu which are directed along the x axis are made now of hybrids built from s and x orbitals. Due to the presence of the phosphine ligands, these two hybrids point toward the internuclear space and are therefore important for the Cu···Cu interaction. As above, each of the two Cu-based orbitals finds a match with a chlorine partner: σ^+ with y^+; σ^- with x^+. It is again clear that, for an acute Cu–X–Cu angle, the overlap $\langle\sigma^+|y^+\rangle$ is larger than $\langle\sigma^-|x^+\rangle$, leading thus to the formation of a Cu···Cu

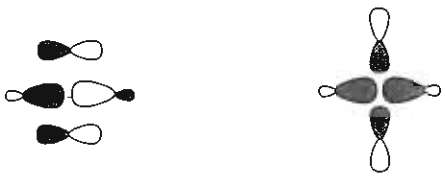

bond when electrons are transferred from X into the Cu orbitals. For a more obtuse angle and for the same Cu–X distances, $\langle\sigma^-|x^+\rangle$ becomes increasingly important and no Cu···Cu bond is made. In this case also, raising the energy of the orbitals of the bridged atoms enhances or decreases Cu···Cu bond formation, depending on the geometry of the system. Here too the energy variation associated with angular change within the rhombus is small because the diminution of a stabilizing interaction is compensated by the increase of another interaction.

In summary, five orbitals are used to build the Cu–X bonds. Three of these interactions (involving σ^+, π^+_y, and π^+_z on Cu) induce the formation of a Cu···Cu bond and thus favor short Cu···Cu distances, while two (involving σ^- and π^-_y on Cu) disrupt the Cu···Cu bond and thus favor long Cu···Cu distances. The outcome of these competing effects is therefore difficult to predict. We wish to show that although precise geometry is impossible to predict, a general pattern of behavior can still emerge.

What are the factors which favor the formation of a Cu···Cu bonding interaction? We have seen that electron transfer into the couples (σ^+, σ^-) and (π^+_y, π^-_y) have unpredictable consequences for the geometry of the rhombus. However, electron transfer into the π_z system is unambiguous, since only π^+_z receives electrons, with the antibonding partner π^-_z remaining empty by symmetry. If the influence of π^+_z dominates, then increased electron donation from the bridged X atoms should lead to a shorter Cu···Cu distance. In order to have π^+_z playing an important role, one should have this orbital as low as possible in energy. Thus, for a stoichiometry $Cu_2(\mu\text{-}X)_2L_2$, L should not be a strong π-donor. This is the case of $Cu_2(\mu\text{-}X)_2L_2$ with L = phosphine, where the shorter Cu···Cu bond is obtained for the better electron-donating bridged atom, I.

Influence of Terminal π-Donor Ligands. If the participation of π^+_z is diminished, a stronger competition occurs between interactions which favor short Cu···Cu distances and those which favor long Cu···Cu distances. This is the case of L with π-donating lone pairs (L = X^-, **2**), since this π-donating effect destabilizes π^+_z. The calculations of $Cu_2X_4^{2-}$ (**2**) with the geometry of $Cu_2(\mu\text{-}Cl)_2P_2$ gives a smaller Cu···Cu overlap population than in the case of $Cu_2(\mu\text{-}X)_2P_2$, which is in agreement with a diminished participation of π^+_z. In addition, we calculate a smaller variation of the overlap population upon changing the energy of the X orbitals in the $Cu_2X_4^{2-}$ systems when compared to $Cu_2(\mu\text{-}X)_2P_2$. This means that electron transfer from X into Cu orbitals occurs equally in Cu···Cu in-phase and out-of-phase orbitals. System **2** is thus especially soft (i.e., associated with a flat potential surface for distortion of the rhombus), and several structures (or a near-continuum) are possible for such systems and intermolecular forces can stabilize the rhombus with a large variety of internal Cu–X–Cu and X–Cu–X angles. In fact, the softness of the $Cu_2X_4^{2-}$ energy surface is evident in the sensitivity of structure to crystal packing forces. Thus, for a rhombus with D_{2h} symmetry, $Cu_2Br_4^{2-}$ has been characterized with Cu···Cu distances of 2.74 and 2.94 Å, depending on the nature of the cation.[7-9] Similarly, $Cu_2I_4^{2-}$ has been characterized with distances between 2.70 and 2.96 Å.[10-12] In each of these examples, there is no especially short cation–anion distance which could be used to explain the large variation in the geometry of the rhombus. If intermolecular forces increase (i.e., the case of close cation–anion contact), values for the Cu···Cu distance can even be very different from the above value. Thus, a distance of 2.66 Å has been observed for the tetrathiatetracenium salt of $Cu_2Br_4^{2-}$,[6] and a record short distance of 2.43 Å has been seen in the $[Cu_4\{5,7\text{-dimethyl}[1,2,4]\text{-triazolo}[1,5\text{-}a]\text{pyrimidine}\}_4Cl_2]^{2+}$ salt containing $Cu_2Cl_4^{2-}$.[2]

The geometry of the rhombus can also undergo another type of distortion: the $Cu_2X_2L_2$ dimer can tend toward separating into two weakly interacting CuXL monomers (**4**).[3,4,13,26] There

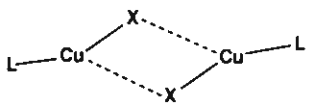

4

are numerous examples of such distortion in the series $Cu_2X_4^{2-}$ and one reported example in the case of $Cu_2I_6^{4-}$.[10-12] The degree of this distortion varies greatly. The reason for a distortion of this sort can be understood from the above analysis. A good overlap between the orbitals of the X bridge and the CuL fragments can be maintained if one Cu–(μ-X) bond becomes shorter and another one longer. This problem is topologically equivalent to that occurring in the classical vs nonclassical ethyl carbocation in which the overlap between H^+ and π_{CC} varies little with the position of H^+ moving parallel to the C–C bond.[27] The difference in energy between the classical and nonclassical cations is thus very small.

There is also another way to diminish the influence of the π^+_z orbital. In $Cu_2(\mu\text{-}X)_2L_4$ (**3**), the additional terminal ligands use π^+_z and π^-_z to bond to Cu. Therefore, π^+_z is even less available for interacting with μ-X than in the case of $Cu_2X_4^{2-}$. The calculation of $Cu_2(\mu\text{-}X)_2(PH_3)_4$ with the rhombus distances and angles of $Cu_2Cl_2P_2$ gives a considerably diminished Cu···Cu overlap population as compared to $Cu_2(\mu\text{-}X)_2(PH_3)_2$, a clear indication of the disruption of a Cu···Cu bonding interaction. In other words, the saturated Cu center (four-coordinate) does not seek additional bonding interaction. A long Cu···Cu distance should be present, which is indeed the case.[14,15] However, for the same reasons as above, there is considerable variation in the geometry of the rhombus. Thus, for $Cu_2X_2L_4$ (L = substituted pyridine) the Cu···Cu distance varies by up to 0.4 Å (X = I) upon change of the substituent at the pyridine. This has been attributed to intramolecular interaction between the bridged atom and the π system of the pyridine ligand.[14] In the case of L = $P(CCR)_3$, two molecules with significantly different Cu···Cu distances (2.747 and 2.872 Å) are found in the unit cell.[15]

Discussion

In the structural comparison of $[Cu(PCy_3)I]_2$ and $Cu(PCy_3)_2I$, it is unusual that the Cu–(μ-I) distance is actually 0.02 Å *shorter* than that involving the terminal iodide. However, since the primarily σ Cu–P bond distance also lengthens (0.055 Å) on going to the more crowded monomer, we feel that both the Cu–P and Cu–I distances of the monomer are influenced by steric effects. At the same time, the bridged Cu–I distances in $[Cu(PCy_3)I]_2$

(26) Toth, A.; Floriani, C.; Chiesi-Villa, A.; Guastini, C. *Inorg. Chem.* **1987**, *26*, 3897.
(27) Nguyen Trong Anh; Eisenstein, O. *Nouv. J. Chim.* **1977**, *1*, 61.

are very similar to those in $Cu_2I_4^{2-}$ and are slightly (0.05 Å) shorter than those involving four-coordinate copper in $[Cu[P(CCPh)_3]_2I]_2$. Moreover, while the Cu–I bond length varies from 2.52 to 2.59 Å on going from $Cu(PPh_3)_2I$[23] to $Cu(PCy_3)_2I$, the Cu–P distances vary by only 0.01 Å; the Cu–P bond is consequently less variable.

The Cu–(μ-X) distances themselves also testify to the presence of X/Cu multiple bonding. When one compares four- and three-coordinate copper (compare $LCu(\mu\text{-}X)_2CuL$ with $L_2Cu(\mu\text{-}X)_2CuL_2$ in Table I and L_2CuX[23] with L_3CuX[28]), both the bridge and terminal Cu–X distances shorten by 0.15–0.17 Å. Also in $LCu(\mu\text{-}X)_2CuL_2$, Cu–X distances are 0.12–0.24 Å shorter to the three-coordinate copper. We believe these trends are due to multiple bonding to three-coordinate copper. Another analysis of the data leads to the same conclusion. If only σ bonding were involved, the quantity $d(H_3C\text{–}I) - d(H_3C\text{–}Cl) = 0.35$ Å would represent the difference in halogen σ (single) bond radii and would thus be equal to $d[Cu\text{–}(\mu\text{-}I)] - d[Cu\text{–}(\mu\text{-}Cl)]$. In fact, this latter difference is 2.57 – 2.31 = 0.26 Å. The Cu–(μ-I) distance is thus short due to more effective σ or π donation. For comparison, note that the Cu–X distances in coordinatively saturated (i.e., Cu–X single bond) $(Ph_3P)_3CuX$ differ by 0.34 Å (iodide distance minus chloride distance).[28]

The above analysis illustrates the very soft potential energy surface for structural reorganization at Cu^I. Much evidence is available for the softness of these structures. While copper is unsaturated as a tricoordinated species and saturated as a tetracoordinated one, it easily adopts an intermediate situation. Cubane type tetramers $Cu_4X_4L_4$ may distort to create one long Cu–X bond at each copper center when L = olefin but retain a symmetric cubane structure when L = phosphine.[29] It was shown that the softness of the coordination around Cu is responsible for several anomalous structures in solid sulfide/Cu^I chemistry as well as for the ionic conduction of Cu^I.[30] It is therefore not surprising to observe this large range of structures for $L_nCu^I(\mu\text{-}X)_2Cu^IL_n$ systems. These systems can be indifferent to certain geometrical distortions due to the fact that a good interaction between the metal centers and the μ-X ligands is maintained for an angular distortion and even for a bond length distortion of the rhombus. These molecules are therefore "soft" with respect to bond angle modification, and a variety of distortions are observed.

We believe however that, in the simple case of $Cu_2(\mu\text{-}X)_2P_2$, the formation of a weak Cu···Cu bond may take place for a strong electron donor X and that this factor may have an important role to play in stabilizing specific structures. This is a consequence of the borderline character of Cu^I (i.e., between transition and main group behavior), in which the metal s and p orbitals are sufficiently diffuse (relative to those of Zn(II) or Al(III)) that direct metal/metal overlap can be competitive with more conventional metal/halide overlap. The fascinating large spectrum of structures for Cu^I is an outcome of these competing effects.

The effect we analyze here is crudely analogous to the Lewis structure analysis of any transition metal compound with a partially filled d block (eq 1). However, the analogous striving

$$Cp(OC)Co \longrightarrow Cp(OC)Co{=}Co(CO)Cp \qquad (1)$$

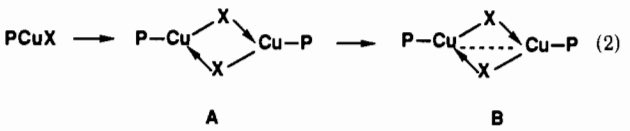

A B (2)

(eq 2) to diminish the unsaturation (16-valence-electron count) in structure A by drawing a Cu/Cu bond, involving only the d block, equally fills both bonding and antibonding MO's. It is only the differential stabilization of the resulting d-based Cu/Cu MO's by the empty metal p_z orbitals (i.e., three-coordinate metal is required) which justifies the Cu/Cu bond drawn in **B**. In the present analysis of the impact on Cu/Cu interaction of varying the μ-X group, it is *partial* occupancy of the metal s and p orbitals which controls the extent to which the intercopper lines drawn in **B** have reality.[31]

Acknowledgment. The Laboratoire de Chimie Théorique is associated with the CNRS (URA 506) and is part of the ICMO and IPCM. This work has been supported by an NSF/CNRS grant for international scientific U.S./France exchange (O.E., K.G.C.) and by a travel grant to G.L.S. from the Academy of Sciences of the USSR.

Supplementary Material Available: Tables of full crystallographic data and anisotropic thermal parameters and figures showing all atom labels (5 pages); listings of observed and calculated structure factors (17 pages). Ordering information is given on any current masthead page.

(28) Barron, P. F.; Dyason, J. C.; Healy, P. C.; Engelhardt, L. M.; Pakawatchai, C.; Patrick, W. A.; White, A. M. *J. Chem. Soc., Dalton Trans.* **1987**, 1099 and references therein.

(29) Håkansson, M.; Jagner, S. *J. Organomet. Chem.* **1990**, *397*, 383. Clot, E.; Håkansson, M.; Jagner, S.; Eisenstein, O. In preparation.

(30) Burdett, J. K.; Eisenstein, O. *Inorg. Chem.* **1992**, *31*, 1758.

(31) It has been reported that solid $(C_5Me_5)_2Ru_2Cl_2(\mu\text{-}Cl)_2$ contains equal amounts of two dimers, with Ru/Ru distances of 2.93 and 3.75 Å. This may be another example of the phenomenon we discuss here for Cu^I. See: Kölle, U.; Kossakowski, J.; Klaff, N.; Wesemann, L.; Englert, U.; Herberich, G. *Angew. Chem., Int. Ed. Engl.* **1991**, 690.